

promoting access to White Rose research papers



Universities of Leeds, Sheffield and York
<http://eprints.whiterose.ac.uk/>

This is a copy of the final published version of a paper published via gold open access in **Annales Geophysicae**.

This open access article is distributed under the terms of the Creative Commons Attribution Licence (<http://creativecommons.org/licenses/by/3.0>), which permits unrestricted use, distribution, and reproduction in any medium, provided the original work is properly cited.

White Rose Research Online URL for this paper:
<http://eprints.whiterose.ac.uk/78602>

Published paper

Walker, SN, Kadiramanathan, V and Pokhotelov, OA (2013) Changes in the ultra-low frequency wave field during the precursor phase to the Sichuan earthquake: DEMETER observations. *ANNALES GEOPHYSICAE*, 31 (9). 1597 - 1603. Doi: 10.5194/angeo-31-1597-2013



Changes in the ultra-low frequency wave field during the precursor phase to the Sichuan earthquake: DEMETER observations

S. N. Walker¹, V. Kadiramanathan¹, and O. A. Pokhotelov²

¹ACSE, University of Sheffield, Sheffield, UK

²Schmidt Institute of Physics of the Earth RAS, Moscow, Russia

Correspondence to: S. N. Walker (simon.walker@sheffield.ac.uk)

Received: 28 March 2013 – Revised: 12 July 2013 – Accepted: 12 August 2013 – Published: 27 September 2013

Abstract. Electromagnetic phenomena observed in association with increases in seismic activity have been studied for several decades. These phenomena are generated during the precursory phases of an earthquake as well as during the main event. Their occurrence during the precursory phases may be used in short-term prediction of a large earthquake. In this paper, we examine ultra-low frequency (ULF) electric field data from the DEMETER satellite during the period leading up to the Sichuan earthquake. It is shown that there is an increase in ULF wave activity observed as DEMETER passes in the vicinity of the earthquake epicentre. This increase is most obvious at lower frequencies. Examination of the ULF spectra shows the possible occurrence of geomagnetic pearl pulsations, resulting from the passage of atmospheric gravity waves generated in the vicinity of the earthquake epicentre.

Keywords. Ionosphere (electric fields and currents; ionospheric disturbances) – radio science (ionospheric physics)

1 Introduction

Electromagnetic phenomena observed in association with increases in seismic activity have been studied for several decades. These phenomena are generated during the precursory phases of an earthquake as well as during the main event. Their occurrence during the precursory phases may be used in short-term prediction of a large earthquake. Perhaps the first observation of perturbations in the surface magnetic field was reported by Moore (1964) at Kodiak a couple of hours before the $M = 9.2$ earthquake that occurred on 27 March 1964. Since then there have been numerous reports of observations of perturbations in the surface magnetic field

associated with seismic activity. Fraser-Smith et al. (1990) reported ultra-low frequency (ULF) magnetic field activity in the frequency range 0.01–0.2 Hz that began around 12 days before the main shock of the Loma Prieta earthquake. Similar observations are also reported by Molchanov et al. (1992) ($M_S = 6$, Spitak), Hayakawa et al. (2006) ($M_S = 8$, Guam), and Prattes et al. (2011) ($M = 6.3$, L'Aquila) amongst others. However, not all large earthquakes exhibit such phenomena. It was reported by Fraser-Smith et al. (1994) that no increases in the ULF wave activity were observed ahead of the the $M = 7.4$ Landers earthquake.

The effects of these electromagnetic precursors perturb not only on the ground electric and magnetic fields but are also responsible for perturbations in the lower D/E regions (Molchanov and Hayakawa, 2008) and upper F region (Liu et al., 2006) of the ionosphere. Within the ionosphere, these electromagnetic precursors are observed over a very wide range of frequency, from DC, ULF to very low frequency (VLF). Most research has concentrated on the observation and identification of waves in the ELF/VLF ranges (e.g. Larkina et al., 1989; Parrot and Mogilevsky, 1989; Chmyrev et al., 1989; Zhang et al., 2009; Akhondzadeh et al., 2010). Using data from the DEMETER satellite, Onishi et al. (2011) identified the occurrence of hiss, whistler mode, and electrostatic turbulence in a search for anomalous variations in wave activity during the period leading up to the Sichuan earthquake. These authors were able to show that the anomalous behaviour in the electrostatic turbulence at a frequency of 20 Hz began about 6 days prior to the earthquake. At low frequencies, in the ULF range a study by Athanasiou et al. (2011) showed evidence for an increase in the energy of ULF waves of up to 360 % for a period of about a month preceding the $M = 7.0$ earthquake that occurred in

Haiti on 12 January 2010 during both day and night-time orbits of DEMETER.

In this paper, the analysis of ULF fluctuations in the electric field as measured by DEMETER in the vicinity of the Sichuan earthquake is presented. The main aim of the French DEMETER microsatellite was to study disturbances of the ionosphere due to seismo-electromagnetic effects as well as various anthropogenic activities. DEMETER occupies a quasi-heliosynchronous (10:30 and 22:30 LT), circular, almost polar orbit with an altitude of 715 km. The satellite performed around 14 orbits per day and was usually operational at geomagnetic latitudes between -65 and $+65$. Thus it provides good coverage in seismically active zones.

The data used were collected by the electric field receiver ICE (Berthelier et al., 2006) on board the DEMETER satellite. The experiment uses four spherical electrodes, each mounted on a 4 m stacer boom to make measurements covering frequencies in the range DC-3MHz in four frequency bands (ULF, ELF, VLF, and high frequency (HF)). In this paper we present observations in the ULF band. The DC/ULF measurements sample the four probe potentials at 39.0625 Hz regardless of operational mode (survey or burst) and filtered with a low-pass 15 Hz filter. The potentials are then combined to provide 3 orthogonal complements of the electric field in the satellite frame. The data from DEMETER are made available via the CDPP data centre in Toulouse (Lagoutte et al., 2006) (<http://cdpp2.cnes.fr/cdpp/login.do>) and also provide auxiliary ephemeris data as well as data to transform the data from satellite frame to geographic and local geomagnetic frames. In this study data collected in survey mode were analysed.

2 Observations

The observations presented in this paper pertain to one specific seismic event, namely the magnitude 7.9 earthquake that occurred in Sichuan, China, on 12 May 2008. Details of this event are given in Table 1. As mentioned in the introduction, there have been numerous reports of seismo-electromagnetic effects observed by orbiting satellites in the ELF, VLF, and HF ranges. In this paper, we concentrate on observations in the ULF wave band. The ULF datasets from the DEMETER ICE electric field instrument contain waveform information in the frequency range below 15 Hz.

2.1 Data coverage

Figure 1 shows the orbital tracks of the DEMETER satellite in the period between 13 March and 19 May 2008. This corresponds to the time period 60 days before to 7 days after the earthquake. The red star shows the location of the epicentre as listed in the online DEMETER catalogue of seismic events. The cyan lines show the orbital tracks of DEMETER during the above-mentioned period. All of the selected orbits

Table 1. Details of the Sichuan earthquake

Time of earthquake	12 May 2008, 06:28
Epicentre	
Latitude	31.02°
Longitude	103.37°
Magnitude	7.9
Depth	10 km

pass within 2000 km of either the earthquake epicentre or its conjugate point determined both at ground level or the altitude of the DEMETER satellite. The black circle encloses a region of radius 1000 km centred on the epicentre location to help provide some sort of scale to the map.

2.2 Variation of ULF wave power along the DEMETER orbit

To investigate the possibility of increased wave noise, the variation of wave power along an orbit was examined. For each orbit the individual spectra were averaged using 30 s time bins and then compared against the average wave power for the whole orbit. An example of the results is shown in Fig. 2, which considers the ULF noise in the vicinity of 5.8 Hz. In the top panel the y axis represents the 30 s time bin along the orbit whilst the x axis represents the days of observation. Since the orbits shown in this figure were measured in the night-time sector (22:30 MLT), the timing bins are numbered south to north. The colour represents the wave power in each 30 s time bin of the orbit as a ratio of the average wave power for the whole orbit. The white stars are used to mark when DEMETER is closest to the earthquake epicentre whilst the black stars mark DEMETER's closest approach to the conjugate point of the earthquake epicentre. The lower panel shows the time of earthquakes with magnitude $M > 4$ that occurred within 1500 km of the Sichuan epicentre within the time period of interest. The large ULF electric field ratios encountered in the regions $y < 5$ and $y > 65$ correspond to high latitudes (south and north respectively). These values are influenced by measurements made within the auroral regions. From this figure it can be seen that the noise measured at this frequency exhibits large changes relative to the background levels around the time that DEMETER flies over the region of the epicentre. In particular, the greatest enhancements around the end of March, mid- to late April, mid-May, and early and mid-June. These periods show enhancements typically 1.5–2.5 times the average level of power for the orbit of which they were observed and around 5–7 times the levels recorded before and after each pass of the conjugate point. The largest of these intensifications also coincide with increased noise levels just north of the southern conjugate point. During the period 12 March to 12 July,

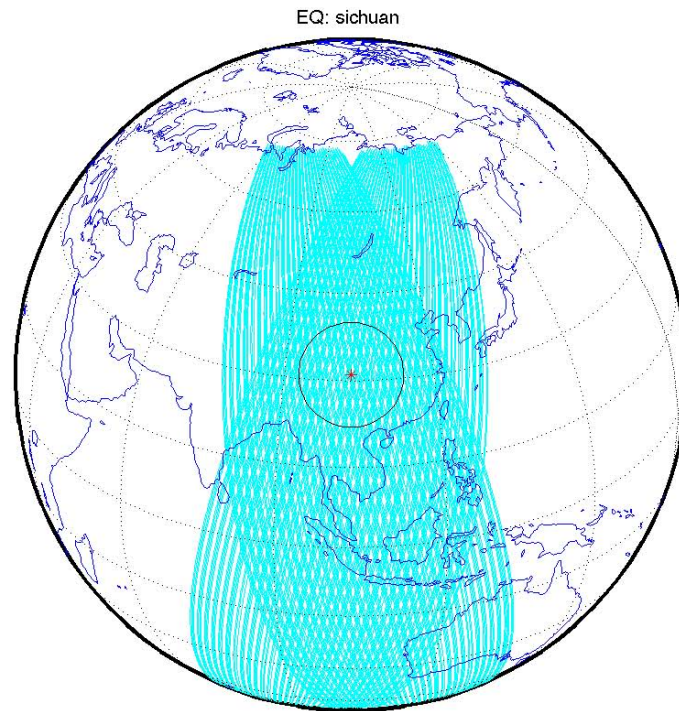


Fig. 1. DEMETER data coverage around the time of the Sichuan earthquake. The cyan lines trace the orbital trajectories that pass closest to the earthquake epicentre (indicated by the red star). The black circle encloses a region of radius 1000 km centred in the epicentre position.

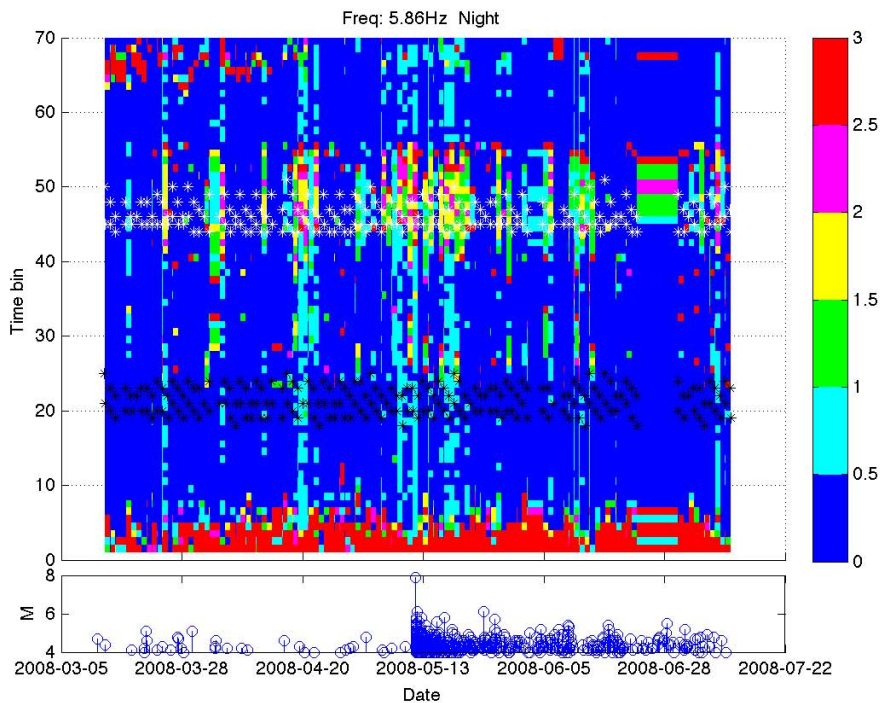


Fig. 2. The upper panel shows the ratio of the variation of the measured ULF wave power averaged into 30 s bins to the mean power measured along a particular orbital track (y axis). The x axis shows the date. The white crosses mark the points in the DEMETER orbit when it passed closest to the epicentre whilst the black indicate the closets passes of DEMETER to the southern conjugate point. The lower panel shows the occurrence time of earthquakes with magnitude $M > 4$ that occurred within 1500 km of the Sichuan epicentre.

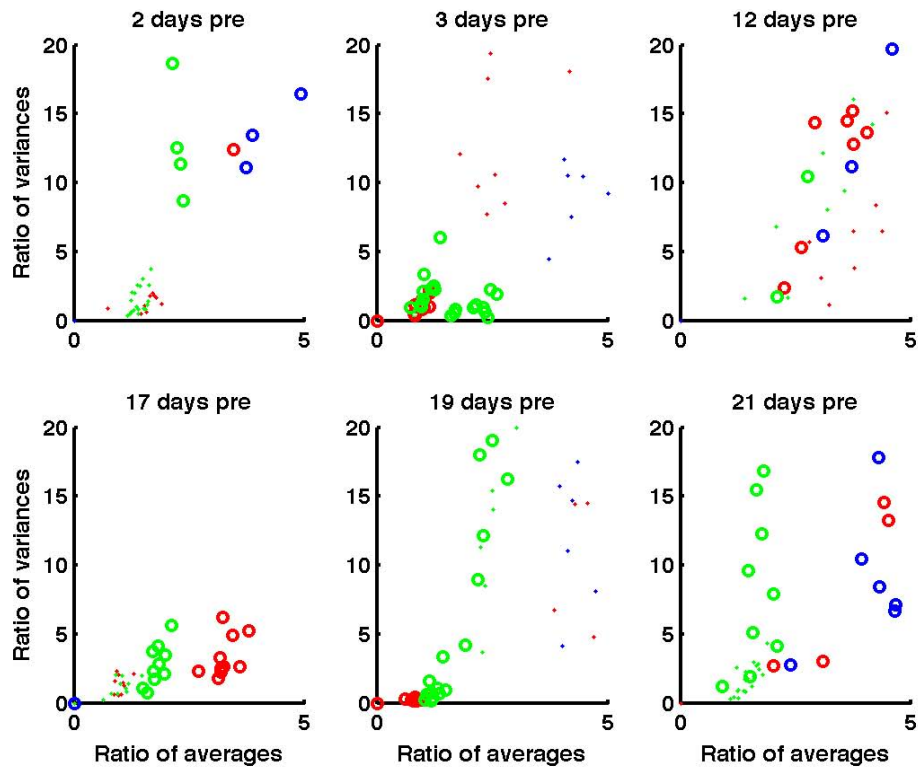


Fig. 3. Ratios of the mean and variance of ULF wave power measured at distances of < 500 km (blue), $500 < D < 1000$ km (red), and $1000 < D < 1500$ km (green) to the wave power measured at distances of $1500 < D < 2000$ km from the epicentre. Daytime passes are shown by the open circles, night-time by dots.

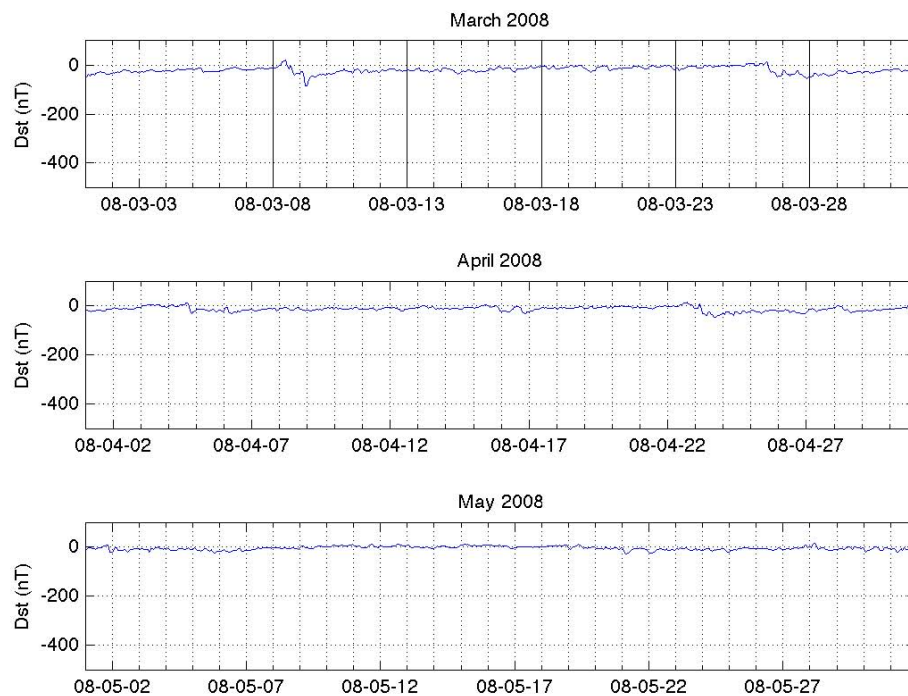


Fig. 4. Variation of Dst for the period 1 March 2008 until 31 May showing the magnetic activity of the magnetosphere for the period around the time of occurrence of the Sichuan earthquake (12 May 2008).

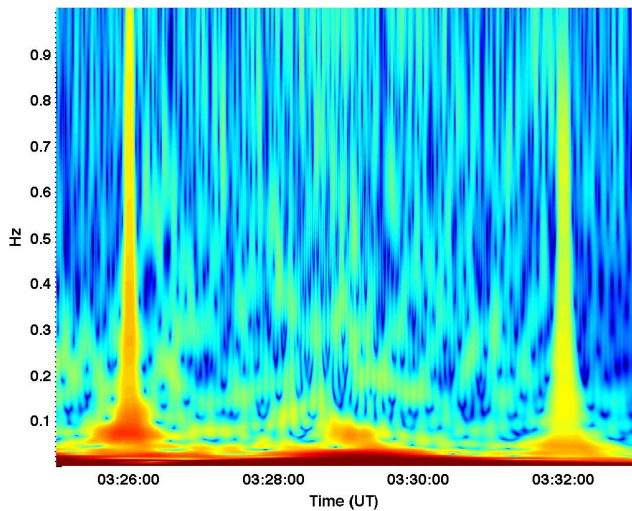


Fig. 5. Low-frequency wave spectrum observed during a passage of the DEMETER satellite in the vicinity of the earthquake epicentre on the day before the earthquake.

the USGS earthquake catalog lists over 1000 events that occurred within a distance of 1500 km of the Sichuan epicentre, of which over 50 had magnitudes $M \geq 5$. These larger events were observed during short periods at the end of March, mid-May after the main event, and early and mid-June. These periods are coincident with the observations of increased wave noise mentioned earlier.

2.3 Variation in vicinity of the earthquake epicentre

The same data were also used to investigate the variation of the mean wave power and its variance as a function of time before the earthquake. Figure 3 shows a number of sequential plots of the variance of the wave power versus the mean wave power in comparison to that measured at distances > 1500 km from the epicentre. The circles represent data from daytime orbits, the dots night-time. The blue symbols represent data collected within 500 km of the epicentre, red between 500 and 1000 km, and green 1000–1500 km. Each set of axes represents a different precursor time before the onset of earthquake. Unfortunately, data at all distances are not available for all precursor times. Most days show a cluster of points almost on the x axis. These points show that there is little variation in the mean wave power over the orbit, and so the plasma wave environment is quite quiet. However, there are occasions when a substantial increase in the wave power and its variance is observed. The largest increases are observed (as would be expected) in the vicinity of the epicentre (blue markers) with the mean wave power reducing as the satellite moves away from immediate region of the epicentre. This effect is obvious when looking at the either the daytime or night-time data alone. It is difficult to compare day and night datasets since the wave activity is actually

quite different on these types of orbits. A few days before the earthquake (in this example 2 days prior), the mean wave power observed in the range $500 < D < 1000$ km increases to that observed closer to the epicentre. Thus it appears that the wave power increases in the vicinity of the epicentre when compared to that measured at larger distances, and so it appears that the increase in ULF noise may be linked to the earthquake precursor wave activity. Figure 3 also shows similar increases in the mean and variance of the observed wave power on other occasions, namely 12, 19, and 21 days before the main event. These periods also exhibited increased wave power in the region of the epicentre and coincide with the increase in seismic activity that resulted in the occurrence of earthquakes whose magnitudes were $M \geq 5$.

3 Discussion

From the observations presented above, it appears that the increase in ULF electric field noise appears to be associated with increased seismic activity. However, these increases may be due to other sources. Therefore it is important to eliminate these as sources for the increase in wave activity discussed above.

Increased levels of plasma wave noise within the inner magnetosphere may result from effects such as magnetic storms and substorms. The state of the magnetosphere may be quantified by a set of geomagnetic indices, in particular the Dst index. Magnetic storms and substorms result from the interaction between the terrestrial magnetosphere and the solar wind. Processes on the surface of the Sun such as coronal mass ejections and solar flares may result in the expulsion of large clouds of particles travelling at high speed. These particle clouds propagate through the inner solar system and, depending upon the direction of propagation, may collide with the Earth's magnetospheric cavity. This increase in the pressure of the solar wind compresses the Earth's magnetic field and, depending upon the orientation of the magnetic field within the particle cloud, injects particles into the magnetosphere via processes such as reconnection. Both of these interactions cause increased electric fields, which result in an increase in the transport of plasma within the magnetosphere via electrical currents. These increased currents will also add to the changes observed in the magnetic field at the surface of the Earth. The magnitude of these changes is usually quantified through the use of geomagnetic indices and in particular the disturbance storm time index (or Dst) (Sugiura, 1991). This index is typically around ± 20 nT during quiet periods. However, during a magnetic storm it may take values in the range -100 nT and below, possible reaching -400 nT in the case of a severe storm. In addition to indicating the onset of the storm, the Dst is also useful in showing how the magnetosphere recovers after such an event. Figure 4 shows the variation of the Dst index during the two-month period leading up to the Sichuan earthquake (12 May 2008).

Throughout this period Dst stays above -100 nT. This value indicates that the magnetosphere is geomagnetically quiet with no storms/substorms occurring. Hence it appears that it is highly unlikely that the increase in ULF electric field strength is due to geomagnetic sources.

A possible second source of this ULF wave noise may result from the effects of ionospheric turbulence triggered by man-made and natural sources of acoustic waves, and this has been widely studied. These events, which can result in the emission of a substantial amount of wave power, can be triggered by either man-made (explosions, rocket launches) or natural (earthquakes, volcanic eruptions, hurricanes, magnetic storms) sources. Such effects have been reviewed in several articles (e.g. Blanc and Rickel, 1989; Liperovsky et al., 2008). Although there are many studies dealing with the influence of large-scale disturbances due to man-made impacts upon the ionosphere, observations of ionospheric turbulence stimulated by such events are rather scarce.

In the acoustic range of spatial-temporal scales, the level of natural ionospheric turbulence is considerably lower than that due to IGWs (internal gravity waves), and therefore the effects due to any man-made sources will be more pronounced. A key step in the investigation of ionospheric turbulence stimulated by an acoustic wave came about as the result of a series of experiments using powerful explosions in Russia and the USA. Typical signatures of waves include a short-lived pulse of localised noise covering a large range of frequencies that are excited as a result of perturbations in the ionospheric plasma. Such a mechanism would not be expected to result in the long-lived increase in ULF noise as observed by DEMETER.

There are two types of wave mentioned in literature that can transport energy from the region of the earthquake epicentre into the ionosphere. One is the vertically propagating acoustic wave mentioned above. The second and more common mechanism involves the propagation of atmospheric gravity waves (AGWs). AGWs have frequencies in the range typically 10 min to 1 h and propagate obliquely to the vertical, resulting in ionospheric perturbations that may cover a large region above the epicentre. Thus it would be expected to observe geomagnetic pulsations (Pc1–Pc5) within the magnetosphere as a result of these AGWs (Hayakawa, 2011). Figure 5 shows the low-frequency (< 1 Hz) dynamic spectrum for a passage of the DEMETER satellite in the vicinity of the earthquake epicentre measured on 11 May 2008 between 03:25 and 03:33 UT. On this particular day, DEMETER passed geographically closest to the epicentre at around 03:28:52 UT (distance 670 km) and was within 200 km of the northern magnetically conjugate point at around 03:30:45 UT. From the spectrogram in Fig. 5, there is clearly an increase in the wave amplitude in the frequency range 0.05–0.15 Hz that has the appearance of pearl-type geomagnetic pulsations, as mentioned by Hayakawa (2011).

4 Conclusions

This paper summarises the results of a study of ULF plasma wave noise observed by DEMETER in the vicinity of the earthquake that occurred in Sichuan, China, in May 2008. This study has shown that there is a probable increase in the ULF wave power in the vicinity of the epicentre. The data also show that the closer to the epicentre, the greater the increase in mean ULF wave power. These effects provide insight into the precursory seismic activity associated with a large earthquake. Indeed, if this is the case, then observations of perturbations in the ionospheric ULF electric fields may have potential use as one of many indicators used to forecast the occurrence of a major earthquake.

Acknowledgements. The research leading to these results has received funding from the European Community's Seventh Framework Programme (FP7/2007–2013) under grant agreement no. 262005. O. A. Pokhotelov is grateful to RFBR (grant no. 11-05-0920) and programme of Prezidium of Russian Academy of Sciences no. 22. SNW is grateful to STFC for financial support.

Topical Editor M. Gedalin thanks two anonymous referees for their help in evaluating this paper.

References

- Akhoondzadeh, M., Parrot, M., and Saradjian, M. R.: Investigation of VLF and HF waves showing seismo-ionospheric anomalies induced by the 29 September 2009 Samoa earthquake ($M_w = 8.1$), *Nat. Hazards Earth Syst. Sci.*, 10, 1061–1067, doi:10.5194/nhess-10-1061-2010, 2010.
- Athanasiou, M. A., Anagnostopoulos, G. C., Iliopoulos, A. C., Pavlos, G. P., and David, C. N.: Enhanced ULF radiation observed by DEMETER two months around the strong 2010 Haiti earthquake, *Nat. Hazards Earth Syst. Sci.*, 11, 1091–1098, doi:10.5194/nhess-11-1091-2011, 2011.
- Berthelier, J. J., Godefroy, M., Leblanc, F., Malingre, M., Menvielle, M., Lagoutte, D., Brochot, J. Y., Colin, F., Elie, F., Legendre, C., Zamora, P., Benoist, D., Chapuis, Y., Artru, J., and Pfaff, R.: ICE, the electric field experiment on DEMETER, *Planet. Sp. Sci.*, 54, 456–471, doi:10.1016/j.pss.2005.10.016, 2006.
- Blanc, E. and Rickel, D.: Nonlinear wave fronts and ionospheric irregularities observed by HF sounding over a powerful acoustic source, *Radio Sci.*, 24, 279–288, doi:10.1029/RS024i003p00279, 1989.
- Chmyrev, V. M., Isaev, N. V., Bilichenko, S. V., and Stanev, G.: Observation by space-borne detectors of electric fields and hydromagnetic waves in the ionosphere over an earthquake centre, *Phys. Earth Planet. In.*, 57, 110–114, doi:10.1016/0031-9201(89)90220-3, 1989.
- Fraser-Smith, A. C., Bernardi, A., McGill, P. R., Ladd, M. E., Helliwell, R. A., and Villard Jr., O. G.: Low-frequency magnetic field measurements near the epicenter of the $M_S 7.1$ Loma Prieta earthquake, *Geophys. Res. Lett.*, 17, 1465–1468, doi:10.1029/GL017i009p01465, 1990.
- Fraser-Smith, A. C., McGill, P. R., Helliwell, R. A., and Villard, O. G.: Ultra-low frequency magnetic-field measurements

- in Southern California during the Northridge earthquake of 17 January 1994, *Geophys. Res. Lett.*, 21, 2195–2198, 1994.
- Hayakawa, M.: On the fluctuation spectra of seismo-electromagnetic phenomena, *Nat. Hazards Earth Syst. Sci.*, 11, 301–308, doi:10.5194/nhess-11-301-2011, 2011.
- Hayakawa, M., Ohta, S., Maekawa, S., Yamauchi, T., Ida, Y., Gotoh, T., Yonaiguchi, H., Sasaki, H., and Nakamura, T.: Electromagnetic precursors to the 2004 Mid Niigata Prefecture earthquake, *Phys. Chem. Earth*, 31, 356–364, 2006.
- Lagoutte, D., Brochot, J. Y., de Carvalho, D., Elie, F., Harivelo, F., Hobara, Y., Madrias, L., Parrot, M., Pinçon, J. L., Berthelier, J. J., Peschard, D., Seran, E., Gangloff, M., Sauvaud, J. A., Lebreton, J. P., Stverak, S., Travnicek, P., Grygorczuk, J., Slominski, J., Wronowski, R., Barbier, S., Bernard, P., Gaboriaud, A., and Walut, J. M.: The DEMETER Science Mission Centre, *Planet. Sp. Sci.*, 54, 428–440, doi:10.1016/j.pss.2005.10.014, 2006.
- Larkina, V. I., Migulin, V. V., Molchanov, O. A., Kharkov, I. P., Inchin, A. S., and Schvetcova, V. B.: Some statistical results on very low frequency radiowave emissions in the upper ionosphere over earthquake zones, *Phys. Earth Planet. In.*, 57, 100–109, doi:10.1016/0031-9201(89)90219-7, 1989.
- Liperovsky, V. A., Pokhotelov, O. A., Meister, C. V., and Liperovskaya, E. V.: Physical models of coupling in the lithosphere-atmosphere-ionosphere system before earthquakes, *Geomagn. Aeronomy*, 48, 795–806, doi:10.1134/S0016793208060133, 2008.
- Liu, J. Y., Chen, Y. I., Chuo, Y. J., and Chen, C. S.: A statistical investigation of preearthquake ionospheric anomaly, *J. Geophys. Res. (Space Physics)*, 111, A05304, doi:10.1029/2005JA011333, 2006.
- Molchanov, O. A. and Hayakawa, M.: Seismo-electromagnetics and related phenomena: History and latest results, TerraPub, Tokyo, 2008.
- Molchanov, O. A., Kopytenko, I. A., Voronov, P. M., Kopytenko, E. A., Matiashvili, T. G., Fraser-Smith, A. C., and Bernardi, A.: Results of ULF magnetic field measurements near the epicenters of the Spitak ($M_S = 6.9$) and Loma Prieta ($M_S = 7.1$) earthquakes – Comparative analysis, *Geophys. Res. Lett.*, 19, 1495–1498, doi:10.1029/92GL01152, 1992.
- Moore, G. W.: Magnetic disturbances preceding the 1964 Alaska earthquake, *Nature*, 203, 508–509, 1964.
- Onishi, T., Berthelier, J.-J., and Kamogawa, M.: Critical analysis of the electrostatic turbulence enhancements observed by DEMETER over the Sichuan region during the earthquake preparation, *Nat. Hazards Earth Syst. Sci.*, 11, 561–570, doi:10.5194/nhess-11-561-2011, 2011.
- Parrot, M. and Mogilevsky, M. M.: VLF emissions associated with earthquakes and observed in the ionosphere and the magnetosphere, *Phys. Earth Planet. In.*, 57, 86–99, doi:10.1016/0031-9201(89)90218-5, 1989.
- Prattes, G., Schwingenschuh, K., Eichelberger, H. U., Magnes, W., Boudjada, M., Stachel, M., Vellante, M., Villante, U., Wesztergom, V., and Nenovski, P.: Ultra Low Frequency (ULF) European multi station magnetic field analysis before and during the 2009 earthquake at L'Aquila regarding regional geotechnical information, *Nat. Hazards Earth Syst. Sci.*, 11, 1959–1968, doi:10.5194/nhess-11-1959-2011, 2011.
- Sugiura, M.: Dst Index, Tech. Rep., Tokai University, available at: wdc.kugi.kyoto-u.ac.jp/dst/dir/det2/onDstindex.html (last access: 23 September 2013), 1991.
- Zhang, X., Qian, J., Ouyang, X., Shen, X., Cai, J., and Zhao, S.: Ionospheric electromagnetic perturbations observed on DEMETER satellite before Chile M7.9 earthquake, *Earthquake Sci.*, 22, 251–255, doi:10.1007/s11589-009-0251-7, 2009.